

## **THERMAL CHARACTERIZATION OF COMMERCIAL ALUMINA WITH DIFFERENT PREPARATION HISTORIES BY EMANATION THERMAL ANALYSIS USING Ra-226 PARENT ISOTOPE \***

TADAO ISHII

*Department of Applied Chemistry, Faculty of Engineering, Hokkaido University, Sapporo 060 (Japan)*

(Received 21 May 1986)

### **ABSTRACT**

Emanation thermal analysis (ETA) using the Ra-226 parent isotope, was applied in the range 25–1450°C for the characterization of commercial alumina powders with various preparation histories. The gas-release stages in the ETA curves for  $\alpha$ -alumina prepared by a Bayer process were broadly grouped into two parts: peak I maximizing at 100–550°C (Ia at about 270–300°C and Ib at 450–500°C) and peak II starting at about 800°C (IIa maximizing at 950°C and IIb at about 1200°C). The effects of Na ions, heating and grinding on the ETA behaviors were discussed.

### **INTRODUCTION**

The author has already reported on the applications of emanation thermal analysis (ETA) for the thermal characterization of iron oxide and aluminum oxide powders [1,2], and for the initial reactivity of metal oxide powders in  $\text{Fe}_2\text{O}_3$ -ZnO and  $\text{TiO}_2$ - $\text{BaCO}_3$  [3,4].

In this paper, the ETA technique, using a surface impregnation method of Ra-226 nuclide, was applied in the range 25–1450°C for characterization of the near-surface of commercial alumina powders with various preparation histories with regard to heating and grinding treatments.

### **EXPERIMENTAL**

The alumina powders with different preparation histories, i.e. heating and grinding treatments, which were produced in a Japanese factory for industrial purposes, were used as the starting materials. For comparison,

---

\* Dedicated to Professor Syûzô Seki in honour of his contribution to Calorimetry and Thermal Analysis.

TABLE 1

Physical properties of industrial alumina prepared by calcining aluminum salt

| Sample No. | Particle size distribution (%) |    |     |    |                        | Primary particle ( $\mu\text{m}$ ) | BET surface ( $\text{m}^2 \text{g}^{-1}$ ) | Na (ppm) | Crystal form                               |
|------------|--------------------------------|----|-----|----|------------------------|------------------------------------|--|----------|--|
|            | -10                            | -5 | -3  | -1 | -0.5 ( $\mu\text{m}$ ) |                                    |  |          |  |
| 18         | 80                             | 60 |     | 20 |                        | 0.3                                | 5  | 10       | $\alpha\text{-Al}_2\text{O}_3$             |
| 19         |                                |    | 100 | 80 | 50                     | 0.3                                | 5  | 10       |  |
| 20         | 90                             | 75 |     | 20 |                        | 0.1                                | 30   | 10       | $\gamma\text{-Al}_2\text{O}_3$<br>(partly) |
| 21         |                                |    | 95  | 70 | 45                     | 0.1                                | 30   | 10       |  |
| 22         | 95                             | 80 |     | 30 |                        | 0.03                               | 100  | 10       | $\gamma\text{-Al}_2\text{O}_3$             |
| 23         |                                |    | 80  | 40 | 20                     | 0.03                               | 100  | 10       |  |

commercial activated alumina (Merck reagent grade,  $-70 + 230$  mesh) was also used. The former is hereinafter called industrial alumina, the latter reagent grade alumina. Tables 1 and 2 show the physical properties of the industrial alumina, which have been taken from a commercial catalog.

The apparatus used for ETA tests is a commercially available Netzsch device (ETA 403–STA 409) for simultaneous ETA–TG–DTA measurements. The standard experimental conditions were as follows: sample weight, 100 mg;  $\text{N}_2$  carrier gas,  $50 \text{ ml min}^{-1}$ ; heating and cooling rate,  $10^\circ\text{C min}^{-1}$ ; threshold, 2 MeV; time constant, 100 s, except Merck reagent grade alumina (300 s). The samples were labeled by a surface impregnation method using Ra-226 solution ( $3 \mu\text{Ci ml}^{-1}$ ) and dried without further washing the surface

TABLE 2

Physical properties of industrial  $\alpha$ -alumina prepared by the Bayer process

| Sample No. | Secondary particle ( $\mu\text{m}$ ) | Primary particle ( $\mu\text{m}$ ) | BET surface ( $\text{m}^2/\text{g}^{-1}$ ) | Density ( $\text{g ml}^{-3}$ ) | $\text{N}_2\text{O}$ (%) | $\text{Al}_2\text{O}_3$ (%) |
|------------|--------------------------------------|------------------------------------|--|--------------------------------|--------------------------|-----------------------------|
| 1          | 60                                   | 5.0                                | 0.6  | 3.96                           | 0.30                     | 99.7                        |
| 2          | 75                                   | 5.0                                | 0.6  | 3.96                           | 0.25                     | 99.7                        |
| 3          | 60                                   | 1.5                                | 3.0  | 3.95                           | 0.30                     | 99.7                        |
| 4          | 60                                   | 0.3                                | 5.0  | 3.94                           | 0.30                     | 99.7                        |
| 5          | 4.0                                  | 4.0                                | 1.3  | 3.95                           | 0.30                     | 99.7                        |
| 6          | 3.2                                  | 0.3–4.0                            | 3.3  | 3.95                           | 0.30                     | 99.7                        |
| 7          | 1.8                                  | 1.5                                | 5.0  | 3.94                           | 0.30                     | 99.7                        |
| 8          | 1.2                                  | 0.3                                | 8.0  | 3.91                           | 0.30                     | 99.7                        |
| 9          | 60                                   | 2.0                                | 1.5  | 3.97                           | 0.05                     | 99.8                        |
| 10         | 60                                   | 2.5                                | 1.0  | 3.97                           | 0.05                     | 99.8                        |
| 11         | 80                                   | 20.0                               | 0.3  | 3.97                           | 0.03                     | 99.9                        |
| 12         | 1.7                                  | 2.0                                | 2.0  | 3.95                           | 0.05                     | 99.8                        |
| 13         | 4.5                                  | 8.0                                | 1.0  | 3.95                           | 0.03                     | 99.9                        |

of labeled powders. Before being used for ETA experiments, in both the first and successive runs, the dried, labeled samples were each stored, for periods exceeding one month until a radioactive equilibrium state was reached.

## RESULTS AND DISCUSSION

### *Interpretation of ETA curves*

A comprehensive review on ETA studies has been reported by Balek [5]. By use of an impregnation method for labeling the sample, Ra-226 nuclide is adsorbed on the surface of the sample and Rn-222 nuclide is formed by its alpha-decay and introduced into the surface layer of the sample by recoil energy. When a state of radioactive equilibrium was reached in the dry labeled-sample, Rn-222 inert gas is distributed in the surface layer, which is about 50 nm thick. Therefore, information obtained from the ETA experiments may be correlated with the behaviors of the near-surface ( $\sim 50$  nm).

Balek [6] proposed that radon release from a dispersed solid may be grouped with temperature rise in three parts: (a) a recoil part,  $E_r$ , due to energy that the radon atom gains during its formation by the decay of radium; (b) a diffusion part,  $E_p$ , due to diffusion in the intergranular space, open micro-pores, etc., of the dispersed powder; and (c) a diffusion part,  $E_d$ , due to bulk diffusion of radon in the solid matrix of the dispersed powder.  $E_r$  is independent of temperature.  $E_p$  is dependent on temperature, and on the dispersity or morphology of the powder, but this is negligible at room temperature.  $E_d$  is dependent on temperature and on the effective surface of a powder.

Matzke [7] showed that the  $E_d$  part of gas release starts at between 40 and 50% of the melting temperature,  $T_m$  (K), for a large variety of ionic crystals of different lattice structures. The onset temperature of gas release for this  $E_d$  part is also similar to that of self-diffusion of the matrix atoms.

From these considerations, in general, the stages of gas release during a linear temperature increase can be grouped according to a temperature of  $(0.4-0.5)T_m$ , at which the self-diffusion of matrix atoms and the bulk diffusion of radon start simultaneously.

Aluminum oxide single crystal ( $\alpha$ -Al<sub>2</sub>O<sub>3</sub>), labeled by the ion-bombardment technique using Kr-85, was selected to demonstrate the gas release stages over the range 25–1100°C by Jech and Kelly [8]. The experimental results were summarized as follows: (1) release starting at 850–1000°C was identified as stage II, occurring at temperatures broadly compatible with self-diffusion, in which the temperatures for the beginning of loop annealing were established; (2) a process maximizing at 700–760°C, which is known to be connected with the amorphous–crystalline transition, has counterparts in the annealing of color-centers and density change; (3) further low-tempera-

ture release at 100–550°C was found to consist, in reality, of two sub-stages, the second of these (maximum at 415–465°C) has counterparts in a variety of annealing phenomena, and is tentatively attributed to excess point defects, and the first sub-stage (maximum at 180–230°C) may possibly involve surface proximity in some way, though comparisons can also be made with the first stage of color-center annealing and with the motion of oxygen interstitials.

On the basis of this useful information, the characteristic changes in ETA curves observed in the present paper were grouped into the following two main stages: stage I at temperatures lower than  $(0.4-0.5)T_m$ , and stage II due to  $E_d$  at temperatures higher than  $(0.4-0.5)T_m$ , 656–889°C for  $\alpha\text{-Al}_2\text{O}_3$ . The ETA peaks corresponding to stages I and II are hereinafter called peaks I and II, respectively. The peak which appears at temperatures of about  $(0.4-0.5)T_m$  was represented as peak I', because in the repeated run this peak showed a behavior similar to that of peak I.

#### *ETA curves of reagent grade alumina*

Figure 1 shows the DTA-ETA curves for a sample of reagent grade alumina. The curves obtained in the first and successive runs are represented by solid and dashed lines, respectively. For sample A10 (original activated alumina (Merck)), the ETA peaks of first-run heating up to 1450°C correspond well with the DTA peaks of dehydration at about 300°C and of the  $\alpha$ -transition at 1250°C, respectively. In the repeated run, the ETA curve becomes typical of  $\alpha\text{-Al}_2\text{O}_3$  with a simple peak II at 1350°C starting at about 800°C; there is no release corresponding to stage I.

For sample A11 ( $\alpha\text{-Al}_2\text{O}_3$ ), which has been prepared as an  $\alpha\text{-Al}_2\text{O}_3$  form by calcining sample A10 at 1300°C for 2 h in air and grinding to pass through 325 mesh sieve, three peaks appear in the following temperature ranges; peak I at 100–550°C, peak I' at 700°C and peak II starting at about 800°C. Further, peak II is split into two peaks: IIa at 1100°C as a shoulder and IIb at 1350°C. Peak IIb agrees with that of typical  $\alpha\text{-Al}_2\text{O}_3$  which appeared in the repeated run of sample A10. It is thought that the appearance of peaks I, I' and IIa results from mechanochemical effects which were caused by the heating and grinding treatments during the preparation of sample A11. In the repeated run, these new peaks, I, I' and IIa, disappear and only peak IIb remains as a stable one. In the third run, peak IIb, similar to that in the second run, appears.

A11(B) shows the results of a stepwise test of sample A11. Peaks I, I' and IIa, due to mechanochemical effects, tend to disappear on annealing at relatively low temperatures.

#### *ETA curves of industrial alumina*

##### *High-purity alumina by calcining aluminum salt*

Figures 2–4 show ETA and TG-DTA results for sample Nos. 18–23,

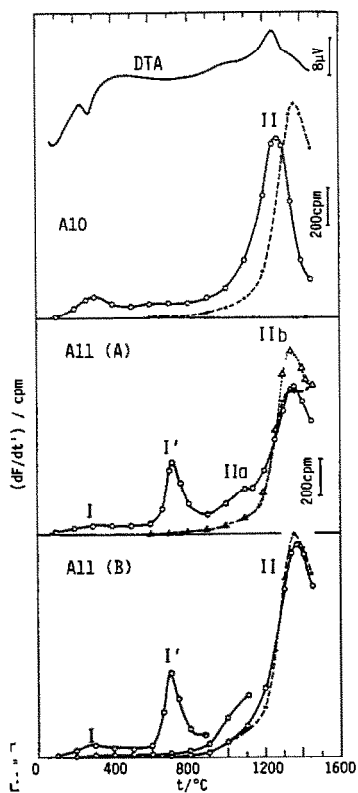


Fig. 1. ETA-DTA curves for reagent grade alumina. A10, activated alumina (Merck); A11(A),  $\alpha$ -alumina prepared by calcining sample A10 at 1300°C for 2 h in air followed by grinding to -325 mesh; A11(B), stepwise tests of sample A11. (○—○) First run; (●- - -●) second run; ( $\Delta$ · · · ·  $\Delta$ ) third run.

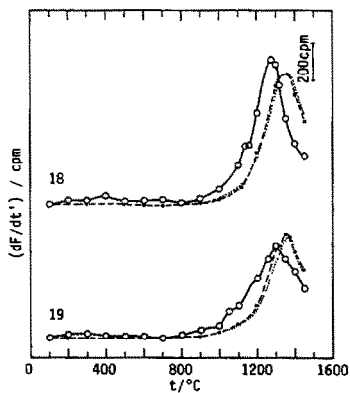


Fig. 2. ETA curves for sample Nos. 18 and 19. (○—○) First run; (●- - -●) second run; ( $\cdot$ · · · ·) third run.

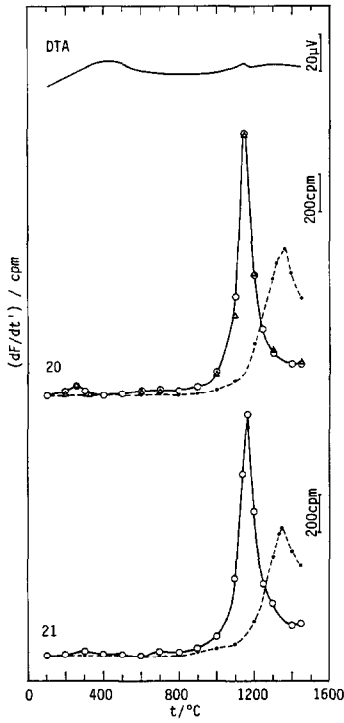


Fig. 3. ETA-DTA curves for Sample Nos. 20 and 21. (○—○) First run; (●- - -●) second run; (Δ) reproducibility test.

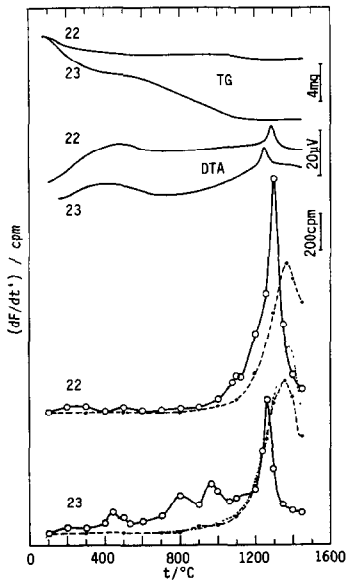


Fig. 4. ETA and TG-DTA curves for the sample Nos. 22 and 23. (○—○) First run; (●- - -●) second run; (· · · · ·) third run.

which were prepared by calcining high-purity aluminum salt. Sample Nos. 19, 21 and 23 were prepared by grinding sample Nos. 18, 20 and 22, respectively, without leading to a serious change of the primary particle size. Sample Nos. 18 and 19 were converted to the  $\alpha$ - $\text{Al}_2\text{O}_3$  form, but Nos. 20–23 were not thoroughly converted. This is due to the use of different calcining temperatures. The DTA curve in Fig. 3 and the TG–DTA curves in Fig. 4 show transitions to  $\alpha$ - $\text{Al}_2\text{O}_3$  behavior.

In Fig. 2, the ETA behaviors of Nos. 18 and 19 may be considered to be in a similar pattern as the reagent grade sample A11 in Fig. 1. Compared with the curve of sample A11 in the first run, the disappearance of peak I' and the shift of peak IIb to the low temperature side are probably due to a difference in preparation conditions (low heating temperature and mild grinding). In Figs. 3 and 4, in general, the ETA behaviors are comparable to that of sample A10 in Fig. 1. A good reproducibility of the ETA curve is shown for sample No. 20 in the same impregnation batch.

The mechanochemical effects of grinding on the ETA curves of Nos. 19 and 21 are not so significant. This is due to the use of such mild grinding that the primary particle was not seriously affected. On the other hand, the ETA curve of No. 23, having a very fine primary particle of  $0.03\ \mu\text{m}$ , greatly differs from No. 22. It is thought that gas release was affected by the dehydration process of water adsorbed during the grinding treatment rather than the grinding itself, considering a large weight decrease for the TG curve of No. 23. All of the curves in repeated runs lead to the typical curve of  $\alpha$ - $\text{Al}_2\text{O}_3$  with a single peak IIb at  $1350^\circ\text{C}$ .

#### *Coarse $\alpha$ -alumina by Bayer process ( $\text{Na}_2\text{O}$ : 0.25–0.3%)*

Figure 5 shows the ETA curves for sample Nos. 1–4, which were prepared industrially by a Bayer process. These samples are characterized by a large secondary particle-size of about  $60\ \mu\text{m}$  and a high Na content of about 0.3% in  $\text{N}_2\text{O}$ . Sample No. 1 resembles No. 2 in primary particle-size and ETA behaviors, but differs from sample Nos. 3 and 4 in primary particle-size and the appearance of peak IIb. Further, the ETA curves for these samples differ significantly, in both the first and successive runs, from those of the reagent grade alumina in Fig. 1 and high-purity industrial alumina in Figs. 2–4. Good agreement between the ETA curves of second and third runs for Nos. 1 and 4 means that a stable release-behavior had been approached in the second run. These results show that the same interpretation as in Figs. 1–4 is inapplicable to the alumina samples prepared by a Bayer process. However, these alumina samples (Nos. 1–4) have a regular release pattern. Hence, the peak-grouping for reagent grade  $\alpha$ - $\text{Al}_2\text{O}_3$  was applied to consider the DTA curves of sample Nos. 1–4.

In the first run, the ETA curves can be broadly grouped into two parts: peak I at  $100$ – $350^\circ\text{C}$  (Ia at about  $270$ – $500^\circ\text{C}$  and Ib at  $450$ – $500^\circ\text{C}$ ), peak II starting at about  $800^\circ\text{C}$  (IIa at  $950^\circ\text{C}$  and IIb at about  $1200^\circ\text{C}$ ). Peak I',

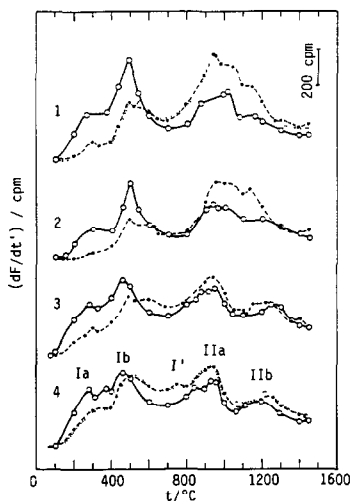


Fig. 5. ETA curves for sample Nos. 1-4. (○—○) First run; (●- - -●) second run; (·····) third run.

at 700°C, appears as a saddle-like shape between peaks I and II. Compared with sample A11 in Fig. 1, peak I is very large and peak II (IIa and IIb) is shifted by about 150°C to the low temperature side. It seems reasonable to assume that such a significant difference from high-purity alumina is mainly due to the effects of Na ions existing in the alumina.

In the second run, all of the peaks in the first run reappear, though there are some changes in their heights. It is noteworthy that peaks I and I' do not disappear in the repeated runs. These ETA results also suggest that Na ions in alumina play a major role in gas release behavior.

#### *Fine $\alpha$ -alumina by Bayer process ( $Na_2O$ : 0.3%)*

Figure 6 shows the ETA curves for sample Nos. 5-8, which were prepared by grinding the coarse samples in Fig. 5 without leading to a serious change of the primary particle size. Sample Nos. 5 and 6 were prepared from No. 1, but the particle size of No. 5 is slightly larger than that of No. 6. Sample Nos. 7 and 8 were prepared from Nos. 3 and 4, respectively.

In the first run, compared with the respective starting sample in Fig. 5, the intensity of peak IIb (at about 1200°C) increases, and peaks Ib (at 450-500°C) and I' (at 950°C) decrease. These peak variations may be attributable to the disaggregation of secondary particles, which are the aggregates of primary particles. However, the ETA curve in the second run reverts to that of the respective starting sample in Fig. 5. It is thought that these interesting phenomena between peaks IIa and IIb are probably due to a reversible grinding-sintering effect between secondary and primary particles. If the gas-release for the Na-bearing samples can be grouped into two parts,  $E_p$  and  $E_d$ , in the same manner as shown in the preceding section on



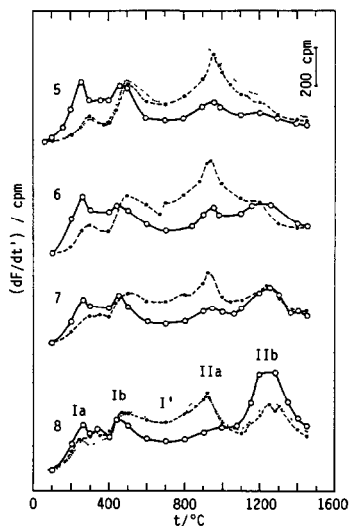


Fig. 6. ETA curves for sample Nos. 5-8. (○—○) First run; (●- - - -●) second run; (· · · · ·) third run.

the interpretation of ETA curves, it is thought that peaks I, IIa and IIb are affected by the Na ions, respectively, situated in positions near the surface, at the grain boundary and in the crystal lattice of the primary particle itself.

*Low-soda  $\alpha$ -alumina by Bayer process ( $Na_2O$ : 0.03-0.05%)*

Figure 7 shows the ETA curves for sample Nos. 9-13, which were

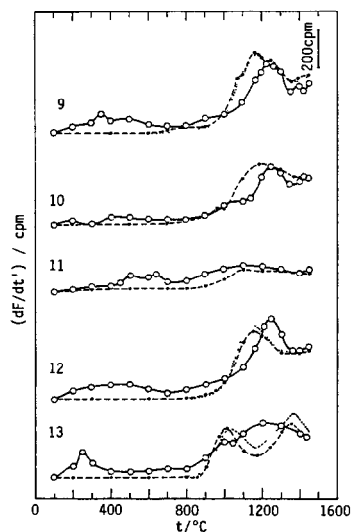


Fig. 7. ETA curves for sample Nos. 9-13. (○—○) First run; (●- - - -●) second run; (· · · · ·) third run.

prepared with an Na-content lower than 0.05% by use of a Bayer process with some additives for accelerating the elimination of Na. Sample Nos. 12 and 13 were prepared by grinding Nos. 9 and 11, respectively. Sample No. 11 has an extremely large primary-particle size. Therefore, this emanating power is low as a whole. The release behaviors for low-soda alumina are intermediate between those of the high-purity alumina from alumina salt and the normal alumina by the Bayer process. This also suggests that Na ions in alumina play an important role in gas release.

#### ACKNOWLEDGEMENT

The author is grateful to Showa Aluminum Industries K.K. for the gift of alumina samples and helpful discussions.

#### REFERENCES

- 1 T. Ishii, *Thermochim. Acta*, 88 (1985) 277.
- 2 T. Ishii, *Thermochim. Acta*, 93 (1985) 469.
- 3 T. Ishii, *Nippon Kagaku Kaishi (J. Chem. Soc. Jpn., Chem. Ind. Chem.)*, (1984) 936.
- 4 T. Ishii, in P. Barret and L.-C. Dufour (Eds.), *Material Science Monographs*, 28A, *Reactivity of Solids, Part A (Proc. 10th ISRS, Dijon, 1984)*, Elsevier, Amsterdam, 1985, p. 959.
- 5 V. Balek, *Thermochim. Acta*, 22 (1978) 1.
- 6 V. Balek, *J. Mater. Sci.*, 17 (1982) 1269.
- 7 H.J. Matzke, *Can. J. Phys.*, 46 (1968) 621.
- 8 C. Jech and R. Kelly, *Proc. Br. Ceram. Soc.*, 9 (1967) 259.